PROTEIN STRUCTURE REPORT

Structure of a mutant human purine nucleoside phosphorylase with the prodrug, 2-fluoro-2′-deoxyadenosine and the cytotoxic drug, 2-fluoroadenine

Sepideh Afshar,[1]*† Michael R. Sawaya,[2†] and Sherie L. Morrison[1]

[1]Department of Microbiology, Immunology, and Molecular Genetics, UCLA-DOE Institute for Genomics and Proteomics, UCLA, Los Angeles, California 90095

[2]Howard Hughes Medical Institute, UCLA-DOE Institute for Genomics and Proteomics, UCLA, Los Angeles, California 90095

Received 12 December 2008; Revised 4 February 2009; Accepted 5 February 2009
DOI: 10.1002/pro.91
Published online 13 February 2009 proteinscience.org

Abstract: A double mutant of human purine nucleoside phosphorylase (hDM) with the amino acid mutations Glu201Gln:Asn243Asp cleaves adenosine-based prodrugs to their corresponding cytotoxic drugs. When fused to an anti-tumor targeting component, hDM is targeted to tumor cells, where it effectively catalyzes phosphorolysis of the prodrug, 2-fluoro-2′-deoxyadenosine (F-dAdo) to the cytotoxic drug, 2-fluoroadenine (F-Ade). This cytotoxicity should be restricted only to the tumor microenvironment, because the endogenously expressed wild type enzyme cannot use adenosine-based prodrugs as substrates. To gain insight into the interaction of hDM with F-dAdo, we have determined the crystal structures of hDM with F-dAdo and F-Ade. The structures reveal that despite the two mutations, the overall fold of hDM is nearly identical to the wild type enzyme. Importantly, the residues Gln201 and Asp243 introduced by the mutation form hydrogen bond contacts with F-dAdo that result in its binding and catalysis. Comparison of substrate and product complexes suggest that the side chains of Gln201 and Asp243 as well as the purine base rotate during catalysis possibly facilitating cleavage of the glycosidic bond. The two structures suggest why hDM, unlike the wild-type enzyme, can utilize F-dAdo as substrate. More importantly, they provide a critical foundation for further optimization of cleavage of adenosine-based prodrugs, such as F-dAdo by mutants of human purine nucleoside phosphorylase.

Keywords: purine nucleoside phosphorylase; X-Ray structure; enzyme substrate specificity; S_N1 mechanism; cancer therapy; immunogenicity; prodrug; cytotoxic drug

---

†Sepideh Afshar and Michael R. Sawaya contributed equally to this work.

Grant sponsor: National Institute of Health Grant; Grant number: RO1 GM074051; Grant sponsor: National Institute of Health Clinical and Fundamental Immunology Training Grant, NIH; Grant number: T32AI07126; Grant sponsor: Howard Hughes Medical Institute.

*Correspondence to: Sepideh Afshar, UCLA, MIMG. 615 Charles E. Young East. 247 BSRB. Los-Angeles, California 90095. E-mail: sepideha@ucla.edu

Introduction

Purine nucleoside phosphorylase (PNP) is a ubiquitous enzyme that catalyzes the reversible phosphorolysis of (deoxy)ribonucleoside to its purine base and (deoxy) ribose-1-phosphate. PNPs are grouped into two main categories based on their molecular weight, subunit composition and enzyme specificity. The first group present in mammals consists of homotrimeric enzymes specific for phosphorolysis of 6-oxo purines (e.g., guanosine). The second group present mainly in prokaryotes consists of homohexameric enzymes that can utilize both 6-oxo and 6-aminopurines (e.g., adenosine).

Because human (hPNP) and *E. coli* PNP (ePNP) exhibit different substrate specificities, efforts have been made to develop adenosine-based prodrugs that can be cleaved by ePNP but not by hPNP. Lack of reactivity of endogenous hPNP with adenosine-based prodrugs, such as 2-fluoro-2′-deoxyadenosine (F-dAdo) means that the administered prodrug is converted to a cytotoxic drug only at tumor sites where ePNP is either expressed[1] or is targeted by fusion to a tumor specific antibody or antibody fragment. Although this makes the ePNP-F-dAdo combination attractive for use in enzyme-prodrug therapy,[1,2] the immunogenicity of the bacterial enzyme and any non-human targeting components preclude their extended use for cancer therapy.

To be effective, the enzyme that converts the prodrug to a cytotoxic drug should not induce an immune response so that multiple rounds of therapy can be administered. At the same time, a wild-type human enzyme cannot be used, because the prodrug would be converted to a cytotoxic drug wherever the endogenous enzyme is expressed causing systemic toxicity. To design an enzyme which circumvents these problems, the substrate specificity of hPNP was altered by introducing two mutations, Glu201Gln:Asn243Asp, in its purine binding pocket. These mutations resulted in an enzyme (hDM) which, unlike hPNP, effectively utilizes (deoxy) adenosine-based prodrugs, such as F-dAdo, 2-fluoroadenosine, and Cladribine as substrates.[3] In addition, hDM can be fused at its C-terminus to a human based tumor targeting peptide without loss of activity.[3] Thus, it should be possible to target hDM to tumors where it would cleave relatively non-toxic prodrugs to cytotoxic drugs with minimal immunogenicity.

In the present study, we have examined the structural changes responsible for the altered substrate specificity of hDM. To elucidate the nature of enzyme interaction with the prodrug, we determined the crystal structures of hDM with F-dAdo and with its cleaved product 2-fluoroadenine (F-Ade) at 2.5 and 2.3 Å resolution, respectively by the molecular replacement method (Table I), using hPNP complexed with guanosine (1RFG) as the model. The structure of hDM with F-dAdo shows that hDM forms hydrogen bond contacts with F-dAdo. Moreover, the structures of hDM with F-dAdo and its cleaved product, F-Ade, give additional insights into the mechanism of catalysis and suggest that additional modifications can be made in the structure of hDM to further optimize its enzymatic efficiency and specificity with adenosine-based prodrugs. Significantly, the structures show that hPNP and hDM are structurally similar, suggesting that hDM will exhibit minimal immunogenicity when used for enzyme-prodrug therapy.

Results and Discussion

Strategy for engineering F-dAdo phosphorylase activity in human PNP

F-dAdo is structurally identical to deoxyadenosine, except for the presence of fluorine at C2 of the purine ring, and is an excellent substrate for ePNP, but is not cleaved by hPNP. Although the human and *E. coli* enzyme share less than 15% sequence identity, their subunit structures superimpose with an RMS deviation of 1.6 Å over 160 aligned α-carbon pairs, and previous mutational studies suggested that only a limited number of amino acid changes would be required to change substrate specificity of hPNP with respect to F-dAdo. Importantly, both enzymes bind purine nucleosides with similar geometry and similar side chains, placing hydrogen bond partners in vicinity of N7 and the N6/O6 of the base. In ePNP and hPNP, these residues correspond to Asp204 and Asn243, respectively. Stoeckler et al. reasoned that introducing aspartate at residue 243 of hPNP should facilitate delivery of a proton to N7 of the purine base to stabilize the negative charge that develops on the base during the transition state.[4–6] The side chain of a second residue, Glu201 in hPNP forms a pair of hydrogen bonds with N1 and N2 of the guanosine base, presumably to aid in orienting the base. Glu201 was mutated to glutamine to balance the charge in the active site and provide a hydrogen bond with N1 and/or F2. There is no equivalent residue in the *E. coli* enzyme, just a network of ordered water molecules.

Overall structure of hDM with F-dAdo

The structure of hDM complexed with F-dAdo is a homotrimer 72 Å in diameter and 65 Å across [Fig. 1(A)]. Each monomer consists of an eight-stranded mixed β-sheet and a five-stranded mixed β-sheet. The β-sheets are connected to the surrounding α-helices by extended loops to form the distorted β-barrel characteristic of human PNP [Fig. 1(A)]. The active trimer is held together by a strong hydrophobic interface. This interface is generated by the interactions of helices F and H containing residues 138–144 and 203–215, respectively from one subunit with helices F and H from the adjacent subunits [Fig. 1(A)]. Because the two mutations Glu201Gln:Asn243Asp were introduced in the purine binding cavity, the global structure of hDM complexed with F-dAdo remains similar to the hPNP complexed with its

Table I. *Statistics of X-ray Data Collection and Atomic Refinement (Numbers in Parentheses Refer to the Outer Shell of Data)*

	F-dAdo	F-Ade
Space group	$P2_12_12_1$	$P2_12_12_1$
Unit cell parameters [Å]	$a = 71.2$, $b = 130.6$, $c = 149.4$	$a = 71.8$, $b = 130.6$, $c = 149.2$
Resolution range [Å]	100.0–2.5 (2.59–2.50)	100.0–2.3 (2.38–2.30)
R_{sym}[a] [%]	9.0 (39.0)	10.5 (33.6)
Number of unique data	47561 (4622)	51620 (1680)
Completeness of data [%]	99.4 (98.1)	81.2 (26.8)
I/σ(*I*)	18.1 (5.1)	16.9 (5.2)
Number of residues/asymmetric unit (3)	847	817
Number of protein atoms	6604	6388
Number of ligand atoms	57	33
Number of sulfate atoms	145	145
Number of water atoms	55	217
Matthews' coefficient [Å^3/Da][b]	3.6	3.6
R [%][c]	20.9 (34.0)	18.5 (26.0)
R_{free} [%][d]	24.8 (41.0)	23.2 (30.0)
Test set size [%], selection	5.0, random	5.0, random
R.m.s. deviations from target values		
Bond lengths [Å]	0.009	0.013
Bond angles [°]	1.3	1.5
Ramachandran angles		
Most favored [%]	91.2	93.5
Additionally allowed [%]	7.7	5.6
Generously allowed [%]	0.4	0.3
Disallowed [%]	0.7	0.6
Errat Overall Quality Factor[%]	93.5	94.0
Verify3D residues with score >0.2[%]	95.6	100.0
Average B factor for protein atoms [Å^2]	54.3	48.3
Average B factor for ligand atoms [Å^2]	73.7	46.0
Average R.m.s. B for protein atoms [Å^2]	1.06	1.68
Average R.m.s. B for ligand atoms [Å^2]	3.21	2.81

[a] $R_{sym} = S|I_o - I_o(mean)|^2/S[I_o^2]$, where I_o is the observed intensity. Both summations involve all input reflections for which more than one symmetry equivalent is averaged.
[b] Matthews' coefficient as defined by Matthews, BW (1968) J Mol Biol 33:491–497.
[c] $R = S||F_o| - |F_c||/S|F_o|$.
[d] R_{free} as defined by Brünger, AT (1992) Nature (London) 355:472–474.

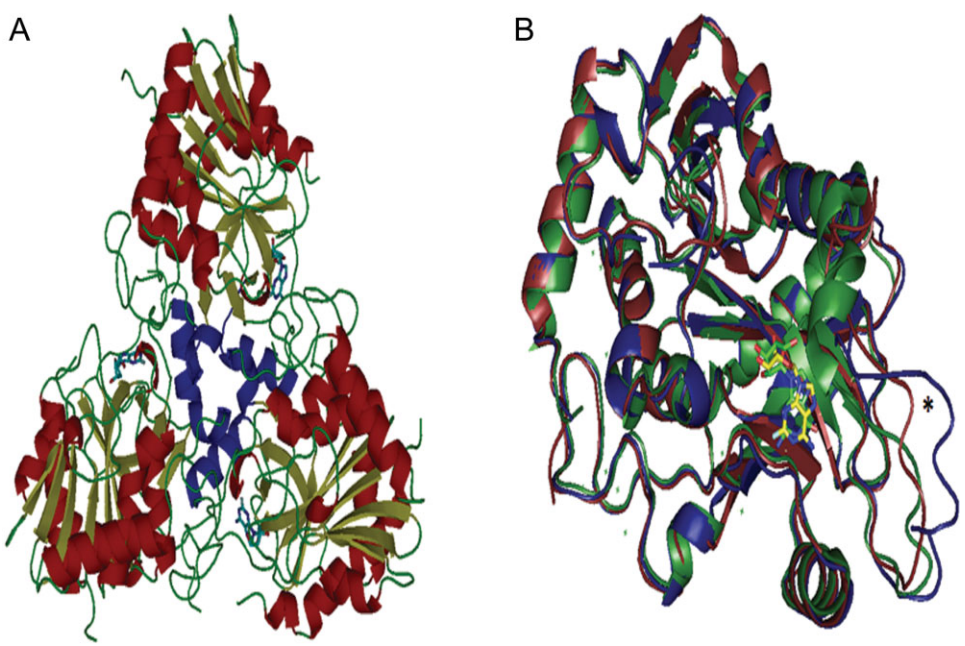

Figure 1. (A) Overall structure of trimeric hDM. In each monomer, β-sheets are in yellow and loops are in green. α-helices are shown in red, except for the two helices F and H of each monomer shown in navy. F-dAdo is shown as sticks. (B) One subunit of hDM complexed with F-dAdo is superimposed on one subunit of hPNP complexed with guanosine (1RFG) and unliganded hPNP (1ULA). hDM is shown in navy, hPNP complexed with guanosine is green, and uncomplexed hPNP is red. In F-dAdo and guanosine, shown as sticks, carbons are in yellow and green, respectively. In both molecules, nitrogens are navy, oxygens red, and fluorine is light blue. The flexible loop, 241–265, is indicated by an asterisk.

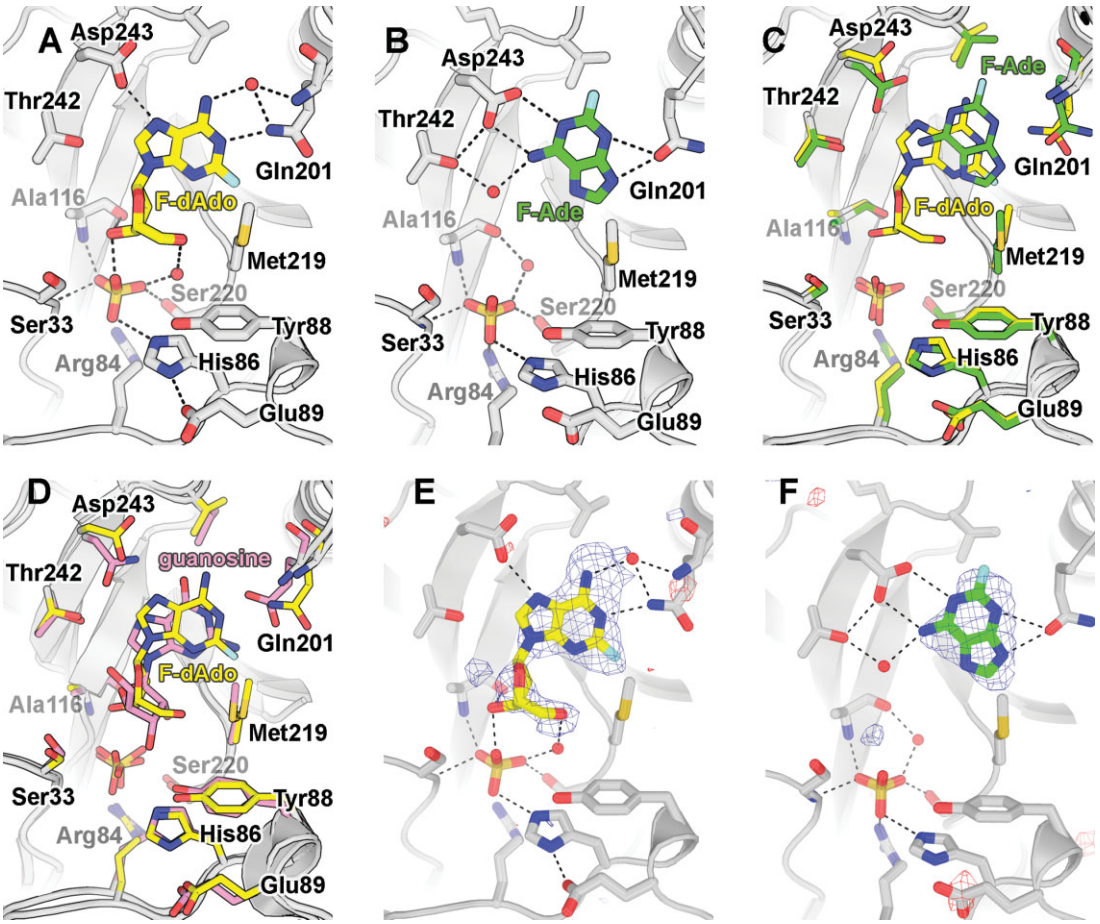

Figure 2. Interaction of hDM with F-dAdo, phosphate/sulfate, and F-Ade. In hDM, carbons are shown in light gray, oxygens in red, and nitrogens in navy. Water molecule is shown as red sphere. In F-dAdo and F-Ade, Fluorine is shown in light blue and carbons in yellow and green, respectively. Sulfate is shown in yellow. (A) A close overview of hDM binding to F-dAdo and sulfate which is bound to the phosphate binding site. (B) A close overview of hDM binding to F-Ade. (C) Base binding pocket of hDM complexed to F-dAdo or F-Ade superimposed. (D) Base binding pocket of hDM complexed with F-dAdo, shown in yellow is superimposed on the structure of hPNP complexed with guanosine, shown in pink (1RFG). (E and F) Simulated annealing F_o-F_c omits maps calculated with CNS.[7] Blue and red contours drawn at +3.5 and −3.5 sigma levels.

natural substrate, guanosine [Fig. 1(B)]. RMS deviation is 0.62 Å for 260 aligned pairs of α-carbons.

Interaction of hDM with F-dAdo and phosphate/sulfate

In hDM, the F-dAdo base binding site consists of residues Val217, Gly218, Phe200, Gln201, Thr242, Asp243, and Lys244 from the same subunit, with the base making hydrogen bonds with two mutated residues Gln201 and Asp243 and π-stacking contact with the phenyl group of Phe200 [Fig. 2(A)]. A water molecule is within hydrogen bond distance of both Gln201 NH2 (2.8 Å) and F-dAdo N6 (2.8 Å) [Fig. 2(A)]. hDM forms a network of hydrogen bond contacts with F-dAdo. Although originally it was hypothesized that for the Asn243Asp mutation the carboxylate group of protonated Asp would form a pair of hydrogen bonds with the 6-amino group and N7 of F-dAdo, we find that only one of these hydrogen bonds is formed with N7 [Fig. 2(A)]. Initially we also hypothesized that two hydrogen bonds would form between the side chain amide group of Gln201 and N1 and 2-fluorine of F-dAdo.[3] Although, we find that Gln201 does form two hydrogen bonds with the base; one hydrogen bond is made with the N1 of F-dAdo, and one bond is bridged by a water molecule [Fig. 2(A)]. The two hydrogen bonds between Gln201 and F-dAdo should result in enhanced binding affinity and indeed the K_M of hDM, was one-third of that observed with the single mutant, Asn243Asp.[3] The ribose binding site includes His86, Try88, Ala116, and Met219 from one subunit and Phe159 from another subunit [Fig. 2(A)]. This hydrophobic pocket locks the ribosyl group in an appropriate orientation for a nucleophilic attack by the adjacent phosphate [Fig. 2(A)].

To inhibit enzymatic activity in the crystal, phosphate, was replaced with sulfate as a precipitating agent. Hence the phosphate binding site, located near the ribosyl group, is occupied by a sulfate ion and is surrounded by Ser33, Arg84, His86, Ala116, and

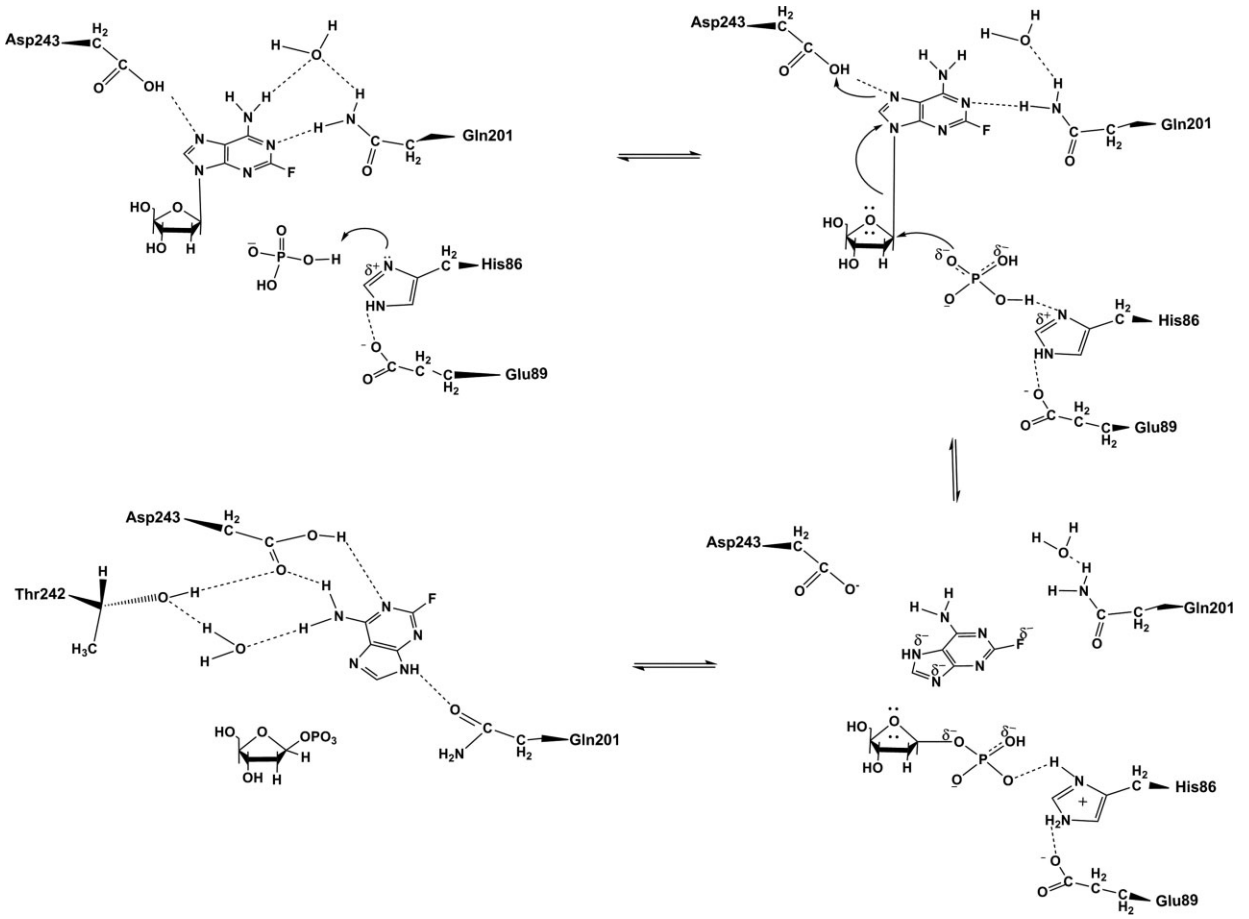

Figure 3. Proposed mechanism for cleavage of F-dAdo to F-Ade by hDM.

Ser220 [Fig. 2(A)]. Ser220 and His86 make hydrogen bond contacts with the sulfate ion through the hydroxyl side chain of Ser220 and imidazole ring of His86, respectively. His86 also makes an additional hydrogen bond contact with the neighboring Glu89 [Fig. 2(A)]. As the result of these interactions, phosphate would be favorably placed not only for its deprotonation by His86, but also to initiate a nucleophilic attack on the ribosyl group.

Interaction of hDM with the cleaved product, F-Ade

Crystals of hDM with the cleaved prodrug, F-Ade, were obtained by incubating crystals of F-dAdo in a low concentration of phosphate for a week. Analysis of the structure reveals that release of ribose-1-phosphate is coupled with a 180° flip of the purine base and movement of the side chains of residues involved in binding to the base [Fig. 2(C)]. As the result, the initial hydrogen bonds present in F-dAdo are replaced with new ones in F-Ade: the side chain amide oxygen of Gln201 forms hydrogen bond with N9, and the carboxyl group of the protonated Asp243 forms hydrogen bonds with N1 and the 6-amino group of F-Ade [Fig. 2(B)]. Movement of Asp243 carboxylate allows formation of a hydrogen bond with the hydroxyl group of neighboring Thr242 [Fig. 2(B)]. This bond between Asp243 and Thr242 was not observed when hDM is in complex with F-dAdo, and may play an important role in optimally positioning Asp243 for making hydrogen bond contact with purine base during catalysis.

Proposed mechanism of phosphorolysis of F-dAdo to F-Ade

Phosphorolysis of purine nucleotides by PNPs proceeds through an S_N1 mechanism by inversion and subsequent cleavage of the glycosidic bond to produce α-ribose-1-phosphate and free purine base.[8] As shown in Figure 2(A), the hydrogen bond contacts between Ser220 and His86 with phosphate lock the phosphate next to a lone electron pair on the His86 imidazole, resulting in phosphate deprotonation. The resulting positively charged His86 might then be stabilized through hydrogen bond contact with the neighboring Glu89. The phosphate dianion initiates a nucleophilic attack on C1′ of the ribosyl sugar, and repels the lone electrons of the endocyclic oxygen of the ribosyl ring (see Fig. 3) resulting in lengthening of the glycosidic bond.[9] As the glycosidic bond lengthens, electrons migrate from the destabilized C-N bond to the purine ring, giving it a formal negative charge that probably localizes at N7, N9 and/or F2 of the base. The

oxocarbenium transition state then resolves into ribose-1′-phosphate.[4,9]

A structural comparison of the substrate and product complexes suggests that conformational changes might occur to stabilize the negative charge that develops on the base during the transition state of the phosphorolysis of F-dAdo. These changes have two points of origin. First, lengthening of the glycosidic bond in the transition state brings N7 of the purine base in hydrogen bond distance with Asp243. Concomitantly the flexible loop, containing residues 241–260, moves to assume a closed conformation, shielding Asp243 from bulk solvent and favoring its protonation.[5] Asp243 subsequently donates a proton to N7 to offset the negative charge that is developed on the base. Consistent with a model which emphasizes the importance of Asp243 is the fact that the Asn243Asp mutation was sufficient to change the substrate specificity of hPNP so that it could accept F-dAdo as substrate.[3]

As the nucleophilic attack by the phosphate dianion is completed, the base flips 180°, such that the carboxyl group of Asp243 now faces the N1 side of the base [Fig. 2(C)]. Flipping of the base results in formation of new hydrogen bonds between Asp243 and N1 and 6-amino group, and between Gln201 and N-9 of F-dAdo [Fig. 2(B)]. Notably, rotation of the base moves N9 of the purine base 4.9 Å away from C1′ of the ribosyl ring, may impose a kinetic barrier to initiate the reverse reaction. Presumably, the formation of new hydrogen bonds would also slow product release.

Alteration of substrate specificity of hPNP

Guanosine is the natural substrate of hPNP. hDM with a *Km* value of 476 μM and *kcat* of 0.0077 s^{-1} has 1.4×10^{-5} fold lower efficiency for converting guanosine to guanine compared with hPNP, indicating that Gln201:Asn243 play a critical role in phosphorolysis of guanosine.[3] hDM utilizes F-dAdo with a *Km* value of 121 μM and an overall efficiency of 533 M^{-1} s^{-1}, but hPNP does not utilize F-dAdo as substrate.[3] The lack of enzymatic activity of hPNP with F-dAdo more probably results from a deficiency in the catalytic step rather than inability to bind F-dAdo, since replacing the mutated Asp243 and Gln201 residues with the wild type Asn and Glu side chains would leave the hydrogen bond pattern unperturbed [Fig. 2(A)]. Presumably, binding of F-dAdo would be equally strong in both hDM and wild type enzymes. However, although ligand binding is necessary, it is not sufficient for enzymatic activity. Indeed, the ribosyl ring can be seen in the structures of hPNP complexed with 6-amino purines, such as adenosine or Formycin A, and these molecules are not phosphorylized.[9]

The increased phosphorolytic activity of hDM toward F-dAdo is more readily explained by the transition state stabilization afforded by the Asn243Asp mutation. Placement of an aspartate at position 243 facilitates protonation of N7 of the F-dAdo base, critical for stabilizing the negative charge that develops on the 6-amino purines during the transition state.[4–6] Although donation of a hydrogen bond to N7 by Asn243 in wild-type hPNP may help to equalize the negative charge dispersed in the ring, it is apparently less stabilizing compared with donating a proton by Asp243. This notion is supported by the fact that mutation of Asn243 to serine, cysteine, and glutamine did not result in any enzyme activity with adenosine.[4] These residues, like Asn243 may form a hydrogen bond with N7 of adenosine, but unlike Asp cannot donate a proton. Despite the fact that glutamate can donate a proton, mutation of Asn243Glu did not produce any activity with adenosine,[4] most probably because of steric differences between Asp and Glu. The role of Asp243 in stabilization of transition state through donation of a proton is further supported by the fact that a sharp decline is observed in adenosine phosphorylase activity in the Asn243Asp mutant at pH values above 7,[4] where Asp243 does not exist in a protonated form. In contrast to 6-amino purines, the lack of a proton donor to N7 is not detrimental to the phosphorolysis of 6-oxo purines as the negative charge is localized at the purine O6, via its enol tautomer, stabilized by hydrogen bond with Glu201.

In addition to the electrostatic contribution to transition state stabilization, hDM mutations might also shift the equilibrium toward a catalytically competent conformation of the active site loop comprised of residues 241–265. The conformational change in this loop results in additional contacts between the enzyme and its substrates, which seems essential for catalysis.[9] Therefore, lack of enzymatic reaction of hPNP with adenosine analogues may be due to lack of necessary contacts resulting from lack of movement in this loop. In fact, comparison of the structures of the unliganded hPNP with hPNP complexed with 6-amino purines (non-substrates) shows no difference in the conformation of this loop (i.e., in both structures the loop is open),[9] which contrasts with what is seen with the structures of hPNP complexed with its natural substrates (the loop is closed over the active site when the natural substrate is bound).[9] In contrast, closure of the flexible loop of residues 241–265 is observed in hDM upon binding of F-dAdo, similar to what is seen with hPNP complexed with guanosine [Fig. 1(B)].

Possibility for further optimization of the rate of phosphorolysis of F-dAdo by hPNP

The rate of phosphorolysis might be improved by altering the prodrug or the active site to shorten the distance between F-dAdo (C1′) and the attacking phosphate dianion. Nucleophilic attack is facilitated by the close approach of C1′ to phosphate (4.0 Å) in the hPNP-guanosine complex (PDB code 1RFG).[10] The distance is even shorter (3.1 Å) in the ePNP-F-dAdo complex where phosphorolysis is known to be exceedingly

efficient.[6] In contrast, the C1′-OPO_3 distance is 5.4 Å, over 2 Å longer in the hDM-F-dAdo structure. Part of the reason for the longer distance in the hDM-F-dAdo structure is the difference in nucleotide conformation; guanosine binds in an *anti* conformation to hPNP, whereas F-dAdo binds in a *syn* conformation to hDM [Fig. 2(D)]. One way to foster the proper orientation of the sugar ring is to use F-Ado as a prodrug rather than F-dAdo. The 2′-hydroxyl on the ribose ring could potentially form a hydrogen bond with the backbone amide nitrogen of Met219, an interaction which cannot occur in the deoxy prodrug. Indeed, introduction of the 2′-hydroxyl improves k_{cat} of hDM more than 3-fold.[3] However, F-Ado is relatively toxic compared with F-dAdo with cytotoxicity observed with CT26HER2/*neu* cells at about 7-fold lower concentrations of F-Ado than of F-dAdo (data not shown), making F-Ado a less suitable prodrug. A second way to foster the proper orientation of the deoxyribose ring would be to place a bulky residue at position 201. A residue bulkier than Gln might rotate the base a few degrees closer to the orientation found in the hPNP-guanosine complex, bringing the deoxyribose closer to the phosphate.

Conclusions

Analysis of the crystal structures of hDM with the prodrug F-dAdo and its cleaved toxic metabolite, F-Ade provides new insights into the interaction of this enzyme-prodrug pair. Our overall goal was to engineer human PNP so that it could effectively cleave adenosine-based prodrugs, including F-dAdo to their toxic purine base. Although we have achieved this goal, it would be desirable to produce more efficient enzymes. The availability of crystal structure of hDM-F-dAdo may facilitate the production of additional rationally designed mutations with enhanced binding and/or catalysis. For example a hPNP that can utilize the clinically available prodrug, Fludarabine may be engineered by modifying the ribose binding site such that it would accept arabinose containing nucleosides as substrate. In addition, the available structure may facilitate design of additional adenosine-based prodrugs that are better substrates for hDM. For instance, F-Ado that has an additional 2′-hydroxyl could aid in bringing C1′ of the ribosyl ring in a closer proximity to dianonic phosphate, making the nucleophilic attack more efficient. In the end, a combination of both enzyme modification with the design of novel prodrugs may be the most effective.

Methods

Expression, purification, and enzymatic activity of hDM

The expression, purification and enzymatic activity of hDM were previously described in detail.[3] Briefly, cultures were inoculated from a single colony, grown at 37°C until an OD_{660} of 0.4–0.6 was reached, at which point the cultures were induced by addition of 1 m*M* IPTG and grown for an additional 4 h at 30°C. To facilitate purification, hDM was fused to an S-tag at its N-terminus. For protein isolation, the bacterial lysate was added to S-protein beads (Novagen; Gibbstown, NJ) and after the beads were extensively washed, the bound protein was eluted with 3*M* $MgCl_2$ and dialyzed against 50 m*M* Tris/HCl, 10 m*M* sodium sulfate and 1 m*M* DTT pH 7.1. Purified protein was concentrated to 87.4 mg/mL for structure determination. Enzymatic activity of hDM with F-dAdo was determined spectrophotometrically by a decrease in absorbance at 260 nm and a concurrent increase in absorbance at 280 nm.

Crystallization

The hDM-F-dAdo complex was prepared by mixing equal volumes of 87.4 mg/mL hDM and 5 m*M* F-dAdo. Crystals of hDM-F-dAdo were prepared by mixing 1.0 μL of protein-prodrug complex with 1.0 μL of reservoir solution in a hanging-drop vapour-diffusion tray at room temperature. The reservoir solution contained 1.54*M* ammonium sulphate, 50 m*M* sodium potassium phosphate, pH 6.8, and 3% trimethylamine N-oxide. Rectangular block shaped crystals appeared in 2 days and grew to full size in about 2 weeks. The largest of these crystals was about 300 microns on an edge. The crystals belong to space group $P2_12_12_1$ (Table I) with unit cell dimensions previously unobserved in hPNP crystals. Crystals were cryo-protected by a quick swipe through a solution containing 70% reservoir and 30% glycerol. F-dAdo at 2.5 m*M* concentration was included in the cryoprotectant to replace any of the F-Ade that formed during crystal growth. The crystal was then immediately cooled to 100 K in a nitrogen cryostream to prevent further conversion to F-Ade. Indeed, the diffraction data used to solve the crystal structure of the product complex, hDM-F-Ade, was simply obtained from a hDM-F-dAdo crystal that lacked the soak with fresh F-dAdo. Apparently the 2 week incubation during crystal growth was sufficient to convert all the initial F-dAdo to F-Ade.

X-ray data collection and refinement

Diffraction data sets were collected at the Advanced Photon Source, beamline 24-ID-C, using an X-ray wavelength 0.9793 Å. An ADSC quantum 315 CCD detector was used to record the data. Data were processed using DENZO/SCALEPACK (Table I).[11] The diffraction was strongly anisotropic for the hDM-F-Ade crystal, extending to 2.3 Å in the b* and c* directions, but only 2.8 Å in the a* direction. Ellipsoidal truncation and anisotropic scaling were performed on the hDM-F-Ade data set as described in Ref. 12. Data statistics for hDM-F-Ade refer to the ellipsoidally truncated data set. The hDM-F-Ade structure was solved using molecular replacement program PHASER[13] and

data to 4 Å resolution. A search model containing a trimer of hPNP molecules was generated from the hPNP-guanosine coordinates, PDB ID 1RFG.[9] Three-fold non-crystallographic symmetry averaging was applied on the electron density map using the graphics program COOT.[14] The model was refined with REFMAC[15] using TLS parameters.[16] In the refinement of the hDM-F-dAdo complex, strong NCS restraints were used initially, and then medium strength restraints were used at the end of the refinement. In the refinement of the hDM-F-Ade complex, medium strength NCS restraints were used initially, and then no restraints were used at the end of the refinement. The geometric quality of the model was assessed with the following structure validation tools: ERRAT,[17] PROCHECK,[18] and WHATIF (Table I).[19] Thr 221 falls in the disallowed region of the Ramachandran plot. However, the electron density map clearly supports the conformation we modeled. The same disallowed conformation is observed in other structures of human PNP (for example, PDB ID 1RFG). Protein structures were illustrated using the program PyMOL.[20]

Coordinates

Protein Data Bank: Coordinates for hDM in complex with F-dAdo or F-Ade have been deposited with accession codes of 3GGS and 3GB9, respectively.

Acknowledgments

The authors thank Duilio Cascio for technical advice and UCLA-DOE Technology Center for use of its crystallization and X-ray diffraction facilities. This work is based upon research conducted at the Northeastern Collaborative Access Team beamlines of the Advanced Photon Source, which is supported by award RR-15301 from the National Center for Research Resources at the National Institutes of Health.

References

1. Voeks D, Martiniello-Wilks R, Madden V, Smith K, Bennetts E, Both GW, Russell PJ (2002) Gene therapy for prostate cancer delivered by ovine adenovirus and mediated by purine nucleoside phosphorylase and fludarabine in mouse models. Gene Ther 9:759–768.
2. Parker WB, Allan PW, Hassan A, Secrist JA, III, Sorscher EJ, Waud WR (2003) Antitumor activity of 2-fluoro-20-deoxyadenosine against tumors that express *Escherichia coli* purine nucleoside phosphorylase. Cancer Gene Ther 10:23–29.
3. Afshar S, Asai T, Morrison SL (2009) Humanized ADEPT comprised of an engineered human purine nucleoside phosphorylase and a tumor targeting peptide for treatment of cancer. MCT 8:1–9.
4. Stoeckler JD, Poirot AF, Smith RM, Parks JRE, Ealick SE, Takabayashi K, Erion MD (1997) Purine nucleoside phosphorylase. 3. Reversal of purine base specificity by site-directed mutagenesis. Biochemistry 36:11749–11756.
5. Koellner G, Bzowska A, Wielgus-Kutrowska B, Luic M, Steiner T, Saenger W, Stepinski J (2002) Open and closed conformation of the *E. coli* purine nucleoside phosphorylase active center and implications for the catalytic mechanism. J Mol Biol 315:351–371.
6. Bennett EM, Li C, Allan PW, Parker WB, Ealick SE (2003) Structural basis for substrate specificity of *Escherichia coli* purine nucleoside phosphorylase. J Biol Chem 278:47110–47118.
7. Brünger AT, Adams PD, Clore GM, DeLano WL, Gros P, Grosse-Kunstleve RW, Jiang JS, Kuszewski J, Nilges M, Pannu NS, Read RJ, Rice LM, Simonson T, Warren GL (1998) Crystallography & NMR system: A new software suite for macromolecular structure determination. Acta Crystallogr D Biol Crystallogr 54:905–921.
8. Bzowska A, Kulikowska E, Shugar D (2000) Purine nucleoside phosphorylases: properties, functions, and clinical aspects. Pharmacol Ther 88:349–425.
9. Erion MD, Stoeckler JD, Guida WC, Walter RL, Ealick SE (1997) Purine nucleoside phosphorylase. 2- Catalytic mechanism. Biochemistry 36:11735–11748.
10. Canduri F, Silva RG, Dos Santos DM, Palma MS, Basso LA, Santos DS, de Azevedo Juniorperiod WF (2005) Structure of human PNP complexed with ligands. Acta Crystallogr D Biol Crystallogr 61:856–862.
11. Otwinowski Z, Minor W (1997) Processing of X-ray diffraction data collected in oscillation mode. Methods Enzymol 276:307–326.
12. Strong M, Sawaya MR, Wang S, Phillips M, Cascio D, Eisenberg D (2006) Proc Natl Acad Sci USA 103: 8060–8065.
13. McCoy AJ, Grosse-Kunstleve RW, Adams PD, Winn MD, Storoni LC, Read RJ (2007) Phaser crystallographic software. J Appl Cryst 40:658–674.
14. Emsley P, Cowtan K (2004) Coot: Model-building tools for molecular graphics. Acta Crystallograph D 60: 2126–2132.
15. Murshudov AAV, Dodson EJ (1997). Refinement of macromolecular structures by the maximum-likelihood method. G.N. Acta Crystallograph D 53:240–255.
16. Winn MD, Murshudov GN, Papiz MZ (2003) Macromolecular TLS refinement in REFMAC at moderate resolutions. Method Enzymol 374:300–321.
17. Colovos C, Yeates TO (1993) Verification of protein structures: patterns of nonbonded atomic interactions. Prot Sci 2:1511–1519.
18. Laskowski RA, MacArthur MW, Moss DS, Thornton JM (1993) PROCHECK: a program to check the stereochemical quality of protein structures. J Appl Cryst 26: 283–291.
19. Vriend G, Sander C (1993) Quality control of protein models: directional atomic contact analysis. J Appl Crystallogr 26:47–60.
20. DeLano WL (2002) The PyMOL user's manual. San Carlos, CA: DeLano Scientific.